Reflection Imaging of EGS Reservoirs at Soultz and Basel using Microseismic Multiplets as a Source

Hiroshi Asanuma[1], Keita Tamakwa[1], Hiroaki Niitsuma[1], Roy Baria[2], Markus Häring[3]

[1]Graduate School of Environmental Studies, Tohoku University, Japan
[2]EGS Energy, UK
[3]Geothermal Explorers Ltd., Switzerland

Keywords

Microseismicity, multiplet, passive reflection, EGS/HDR reservoir

ABSTRACT

The authors have been developing a new variation of passive reflection technique, where microseismic multiplets are used as a source (multiplet reflection imaging using microseismicity: multiplet RIM). Closely similar waveform and precisely determined hypocenter of the multiplet can be effectively used to image structures inside/around the seismically activated EGS reservoirs. In the multiplet RIM, artifacts and blurred reflection image due to limited number of sources and detectors is suppressed by identification of relative/absolute time of arrivals of reflected phase from the multiplets and new concept of inversion.

The multiplet RIM has been applied to a data set collected at Soultz, France and Basel, Switzerland. The coherence index, which is a measure of arrival of reflected phase in the multiplet RIM, suggested that coherent reflected phase among the multiplets were successfully identified. The reflection image showed that there are possible reflectors at the bottom of shallow reservoir and surrounding zone at Soultz. Pre-existing fault around 1200m away from the stimulated zone was imaged at Basel. The indices of reflectivity along a borehole at both the sites were consistent with results from logging.

Introduction

Techniques which enable us to delineate structures inside granitic basement are of importance for development and monitoring of EGS reservoirs. However, in practice, conventional seismic techniques, which have been mainly developed in oil industries, have insufficient ability for this purpose in most of the cases. This is because of high reflection coefficient at the top of the basement and strong attenuation in overburden with a thickness of several kilometers. While, high temperature, pressure, and geothermal liquid and gas inside/around the reservoirs avoid deployment of downhole source or detector for VSP and crosshole measurement.

Soma et al. (2002) have developed a reflection method, which uses natural or induced microseismic events (acoustic emission: AE) as a source (AE reflection method), and its capability for imaging structures inside and around the hydraulically stimulated reservoir at Soultz, France, has been successfully demonstrated. Reflected waves are identified by evaluation of linearity of three dimensional motion of the seismic wave (hodogram) at an observation point and diffraction stack migration is used to obtain reflection image in the AE reflection method. One of the significant advantages of the AE reflection method is that downhole triaxial monitoring of the microseismic signals at one station enables reflection imaging. However, ellipsoidal reflectors appear because of limited number of sources and detectors, and, therefore, techniques to image structures with higher reliability has been expected.

We commonly observe groups of microseismic events which have highly close waveforms despite of their origin time and magnitude. Such events are referred to as “microseismic multiplet” and coherence-based relative phase picking and relative mapping technique of their hypocenters have been developed (Moriya et al., 1994). It has been accepted that the relative hypocentral location of the multiplets are more precisely determined because relative time of arrival among the events can be estimated with high accuracy in the frequency domain.

The authors have been trying to incorporate characteristics of the microseismic multiplets in principles of the AE reflection method, because highly similar waveforms of the multiplet can be used like a “repeatable source” and precisely determined relative hypocenters would improve reliability of reflection image. In this paper, we describe principles behind the “multiplet reflection imaging using microseismicity (multiplet RIM)” and its application to a dataset collected at Soultz, France and Basel, Switzerland.

Principles of the Multiplet RIM

The concepts of the original AE reflection method and the multiplet RIM are compared in Figure 1. In both methods, time of arrival and state of polarization of the direct arrival and the reflected phases are estimated by the analysis of 3D hodogram. Principles of the signal processing and migration in the multiplet RIM is schematically shown in Figure 2. Detail of the main procedures is described below.

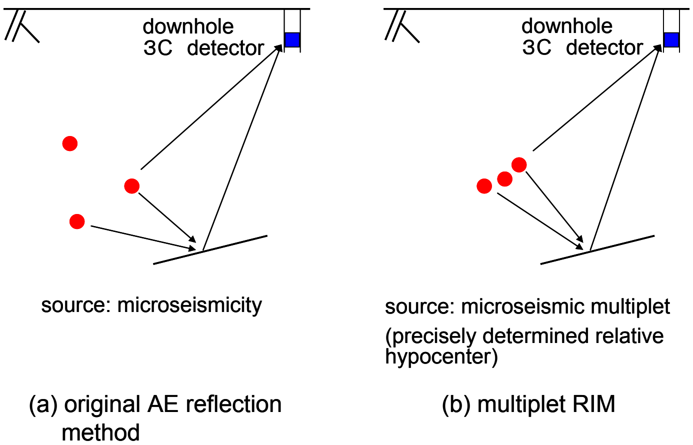

Figure 1. Concepts of the original AE reflection method and the multiplet RIM.

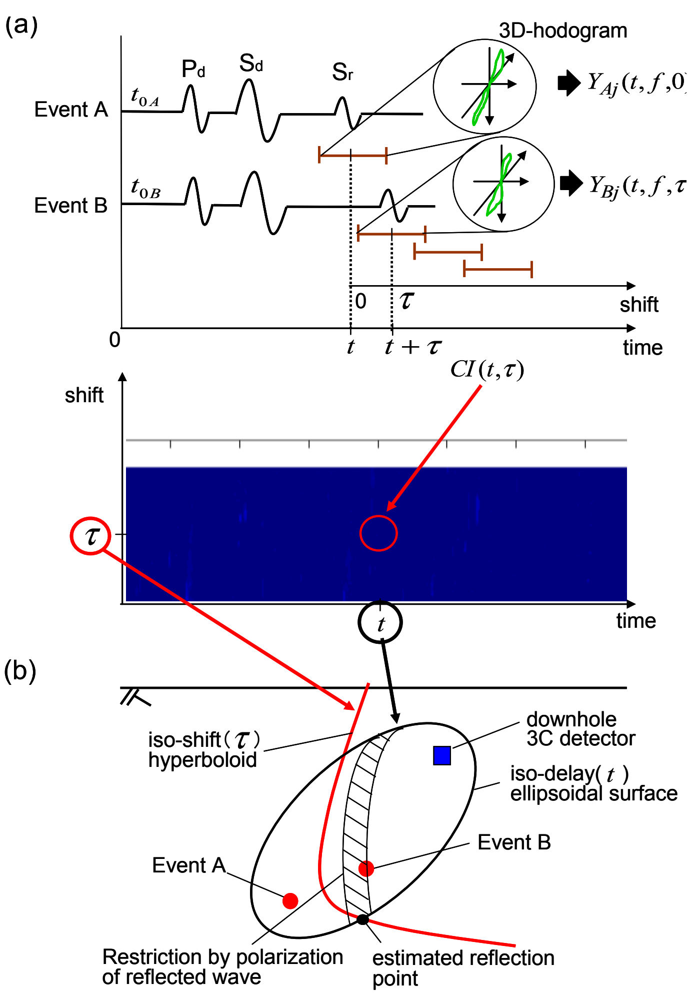

Figure 2. Principles of the multiplet RIM. (a) identification of reflected phase. (b) inversion.

(a) Identification of Reflected Phase

It is assumed that the state of polarization of the 3D hodograms of reflected waves from one reflector has close similarity among microseismic multiplets. Meanwhile, there is a difference in the time of arrival of the reflected wave, because the distances from the hypocenter to the reflector are unique for each event.

Spectra $S_{ij}(t,f,\tau)$(i: event identification, j : component identification) are estimated using a short-time Fourier transform for one pair of the multiplet set. We evaluate the similarity of the 3D hodogram in the time and frequency domains using a 3D time-frequency coherency (3D-TFC) function (Asanuma et al., 2001). Here, we calculate the 3D-TFC function shifting a window for one event by τ for every window time t. The 3D-TFC function used in the multiplet RIM, thus, has three parameters; time t in the reference event, frequency f , and shift τ relative to the reference event, and it is represented as,

$$E_{AB}(t,f,\tau)=1-\frac{\sum_{j=1}^{3}\left\{\frac{Y_{Aj}(t,f,0)}{L_A}-\frac{Y_{Bj}(t,f,\tau)}{L_B}\right\}^2}{2^2}\ . \qquad (1)$$

$Y_{jA}(t, f, 0)$ and $Y_{jB}(t, f, \tau)$ in Eq.(1) are represented by Eq. (2). A set of $Y_{ij}(t, f, \tau)(j=x, y, z)$ draws a 3D ellipsoid (Asanuma et al., 2001). L_A and L_B in Eq.(1) are norms of the 1st eigenvectors of the ellipsoid.

$$Y_{ij}(t,f,\tau)=\left|S_{ij}(t,f,\tau)\right|e^{2\pi ft+\angle S_{ij}(t,f,\tau)}\ . \qquad (2)$$

The 3D-TFC function $E_{AB}(t, f, \tau)$ reaches 1 when both the arrival time t and the shift τ coincide with those of the reflected phase. A coherence index, which is an integration of the 3D-TFC function along frequency using a threshold, is used as an input to the migration. The coherence index $CI(t, \tau)$ is represented as,

$$CI(t,\tau)=\int_{f_{\min}}^{f_{\max}} R(t,f,\tau)\,df\ , \qquad (3)$$

The polarization direction of a reflected wave can be estimated by the 1st eigenvector of the spectral matrix (Niitsuma et al., 1995).

(b) Inversion

An "iso-relative-delay" surface for a reflected phase in a pair of multiplets draws a hyperboloid, and an ellipsoid is also defined as an iso-delay surface in the same manner as the diffraction stack migration. This means that two ellipsoids and one hyperboloid are defined for a reflected phase in a pair of the multiplet. The intensity of the coherence index $CI(t, \tau)$ is migrated onto each hyperboloid and ellipsoids, and a product of the three images becomes an output.

In the inversion, we can restrict the possible location of the reflectors using the polarization of P and S waves and propagation direction of the reflected phase simply assuming P-P and S-S reflections.

In the AE reflection method, the linearity index, which is a measure of the intensity of the linearly polarized reflected phase, is a positive function, and diffraction stack migration is introduced. Hence, the resultant reflection image from microseismic events with limited spatial distribution tends to show an ellipsoidal shape of reflectors. The multiplet RIM on the other hand has an ability to image reflectors more accurately, because the iso-delay and iso-relative-delay surfaces for one reflected wave overlap in a very limited zone after restriction in the polarization direction (see Figure 3).

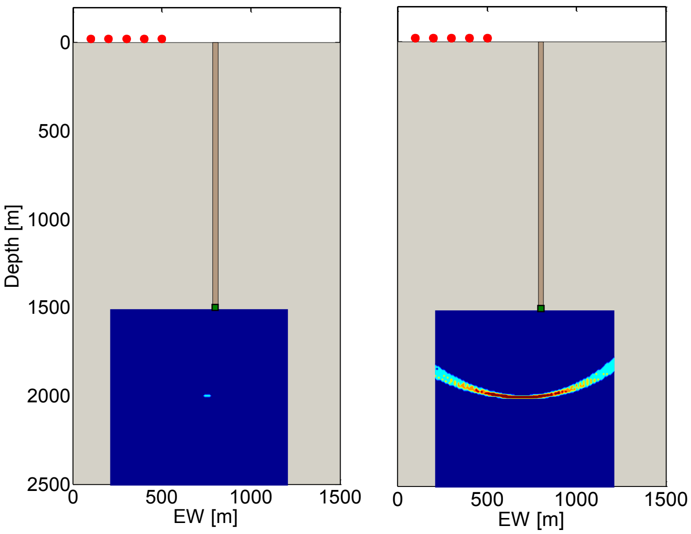

Figure 3. Comparison of a reflection image by multiplet RIM (left) and diffraction stack migration (right) from synthetic study. A planer reflector at (660-740m, 2000m) was assumed.

Application to Field Data

a) Soultz, France

The multiplet-RIM has been applied to a microseismic data collected at Soultz, France in 2003 (Asanuma et al. 2004). The authors have evaluated detect-ability of the 3D hodogram for all the monitoring stations using spectral matrix and concluded that a station 4550 had a reasonable detect-ability of hodogram in a frequency range up to 200Hz.

The multiplets were identified in a frequency range of 100-150 Hz using full trace, because closely coherent events would bring better reflection image. Total number of 861 events (approximately 11% of located events) was identified as a multiplet for the multiplet RIM. An example of identified multiplet is shown in Figure 4.

The hypocentral location of the multiples were determined by double difference (DD) method after manually picking relative time of arrivals of P and S waves for each cluster. Absolute location of each multiplet was determined in reference to a center of gravity estimated by joint hypocenter determination in this study. The hypocenters were distributed in a depth range of 4000-5500 m. An example of coherence index for a pair of multiplet is shown in Figure 5. Higher coherence indices show presence of direct arrivals and reflected phase.

Reflection images by the multiplet RIM and diffraction stack migration of instantaneous envelope are shown in Figure 6. The multiplet RIM resolved some reflectors around at the bottom on shallow reservoir (-3500 m), while the diffraction stack migration drew blurred ellipsoidal reflector. Higher reflectivity appeared at west of stimulated zone at depth around 3000-3500 m in a image by the multiplet RIM is currently considered as an artifact by restriction in the polarization direction.

Coherence index along a borehole GPK-1 is compared with fracture density identified from FMI and temperature gradient from PTS logging in Figure 7. The coherence index is closely correlated to fracture density and highly permeable zone around a depth of 3500m, demonstrating that the multiplet RIM has an ability to identify fractures in the granitic basement.

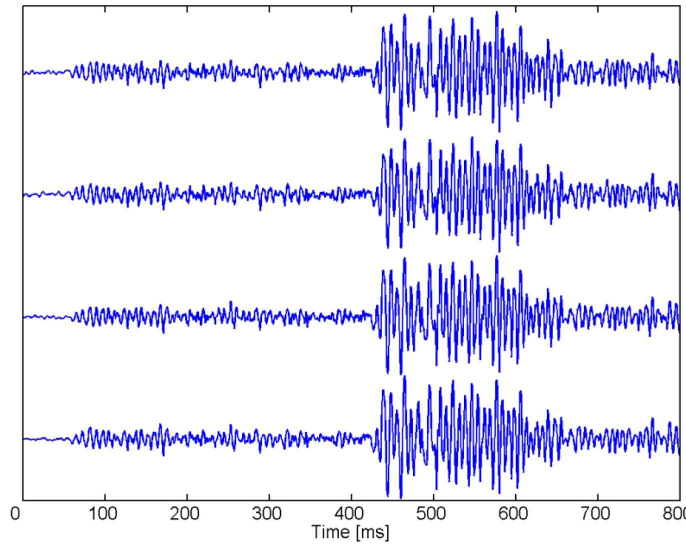

Figure 4. An example of identified multiplet recorded at Soultz.

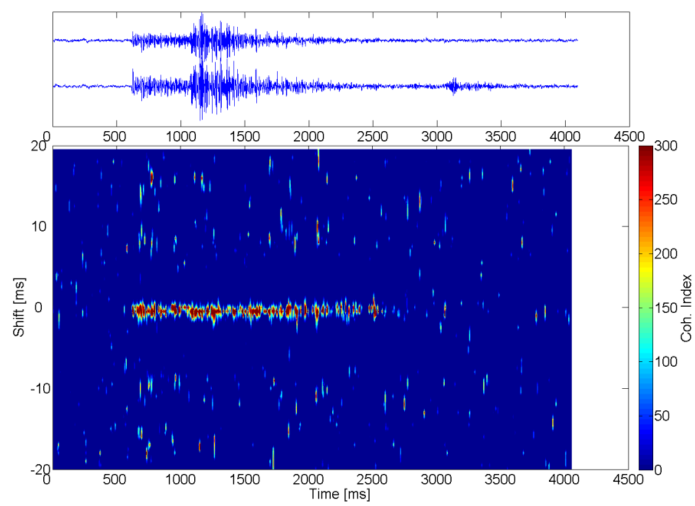

Figure 5. An example of coherence index for a pair of multiplets recorded at Soultz.

b) Basel, Switzerland

Total number of 1407 microseismic multiplets were used as input for reflection imaging at Basel. After evaluation of linearity of the 3D hodogram in the frequency domain, we used signals from stations Otterbach2, Haltingen, and St.Johann (Asanuma et al., 2007). An example of coherence index for a pair of multiplet is shown in Figure 8.

Reflection image obtained by the multiplet RIM is shown in Figure 9, where EW vertical slice at 100m south of injection well Basel-1 is shown. Higher reflectivity appeared around the cloud

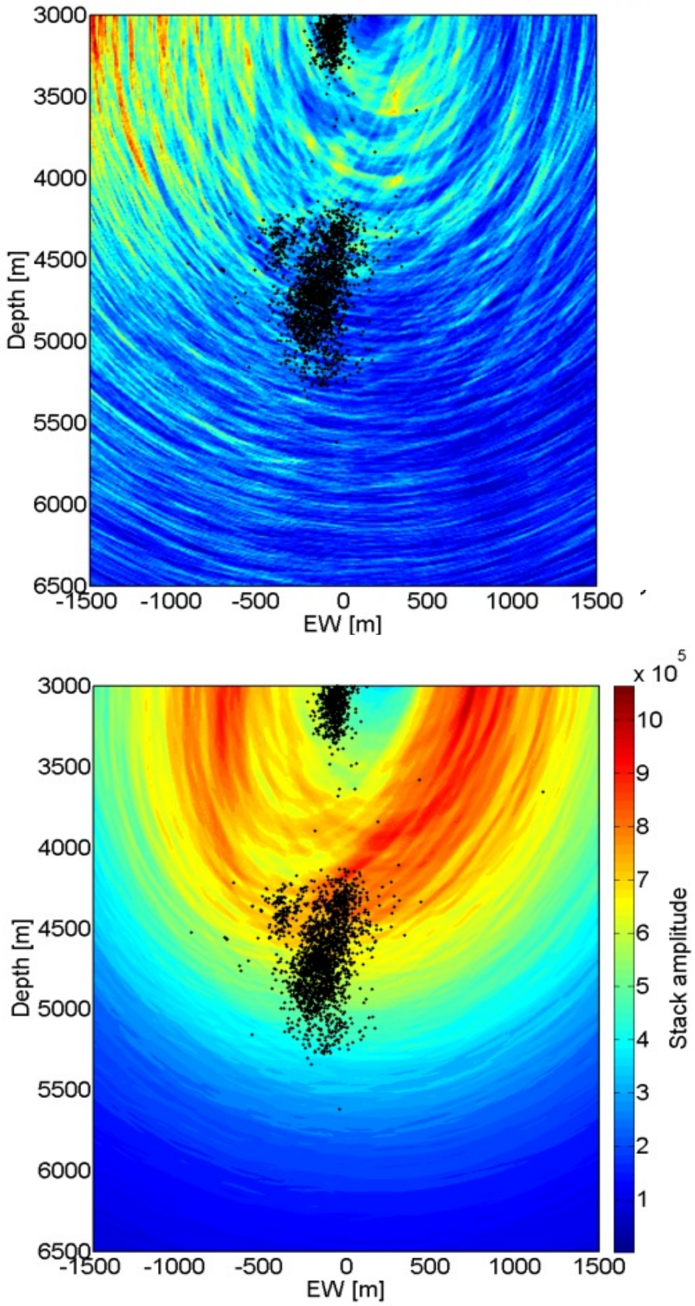

Figure 6. Reflection images at Soultz by the multiplet RIM and diffraction stack migration of instantaneous envelope. Top: multiplet RIM. Bottom: Diffraction stack of instantaneous envelope.

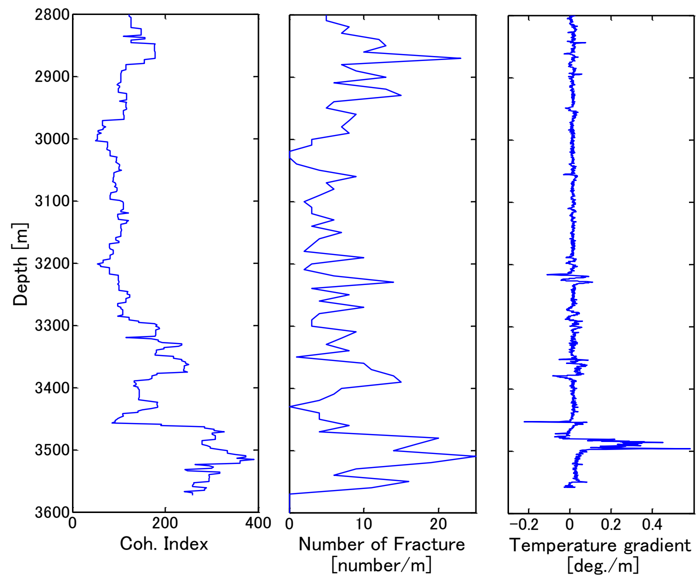

Figure 7. A comparison of coherence index from the multiplet RIM, fracture density identified from FMI, and temperature gradient along a borehole GPK-1, Soultz.

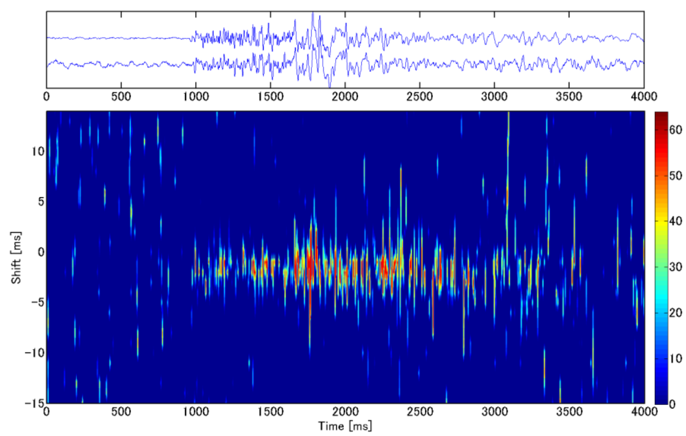

Figure 8. An example of coherence index for a pair of multiplets recorded at Basel.

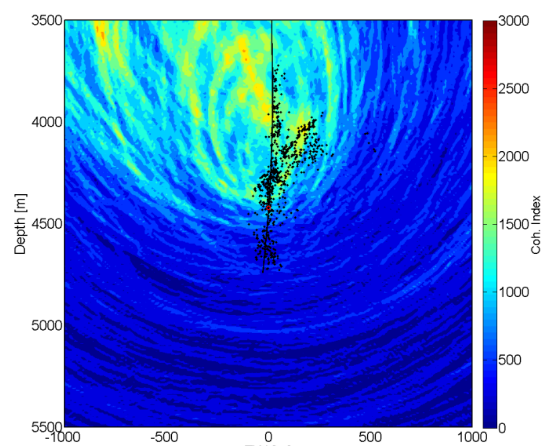

Figure 9. Reflection images at Basel by the multiplet RIM

of hypocenters. This would correlates to a difference in acoustic impedance inside of the stimulated zone from virgin state. A vertical slice (EW-depth) at 300m south of Basel-1 is compared with a reflection image obtained by Fresnel volume migration where mirror reflection is assumed (Reshetnikov et al., 2011) in Figure 10. The two reflection image from independent processing techniques show good agreement suggesting that existing fracture or fault at 1200m east of the injection well has been identified.

Coherence index along the injection well Basel-1 is shown with fracture density, ultrasonic traveltime, and Gamma ray in

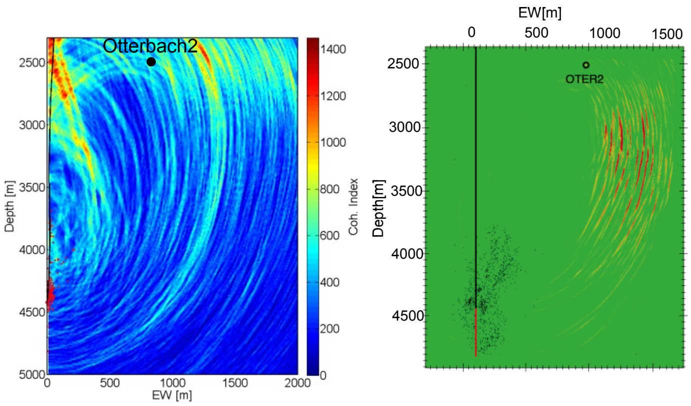

Figure 10. Reflection images at Basel by the multiplet RIM and Fresnel volume migration. Left: multiplet RIM. Right: Fresnel volume migration.

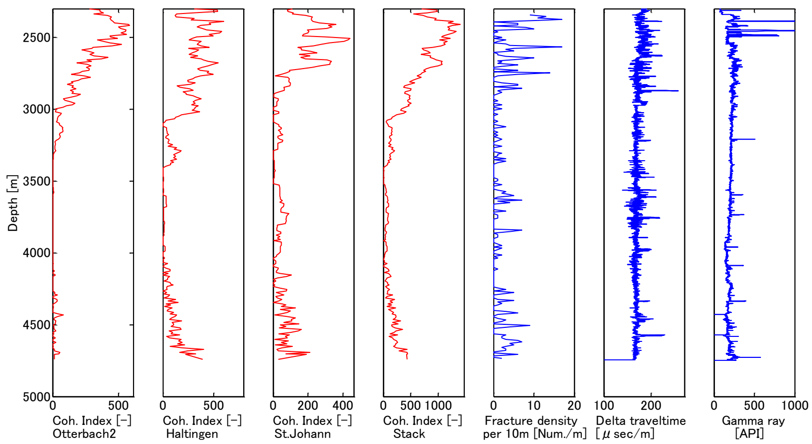

Figure 11. A comparison of coherence index from the multiplet RIM, fracture density identified from FMI, traveltime from sonic log, and Gamma ray along a borehole Basel-1, Basel.

Figure 11. The coherence indices from the signals detected by three stations show reasonably good correlation to the logging data in this case.

Conclusions

The authors have described principles behind a new microseismic reflection technique using microseismic multiplets as a source. Identification of absolute and relative time off arrivals of reflected phase are estimated by an analysis of 3D hodogram in the time and frequency domains, and this enables us to image structures with better resolution/reliability than conventional diffraction shack migration with a few numbers of stations.

It has been demonstrated from the analysis of microseismic data collected at Soultz and Basel that the multiplet RIM has an ability to estimate existing fractures inside the granitic basement and structures around the stimulated zone. We, hence, conclude that the mutiplet RIM can be effectively used to image structures around the stimulated zone inside granitic basement, although further studies to improve reflection image should be made.

Acknowledgements

Part of this work is supported by JOGMEC and Grant-in-aid for Scientific Research, JSPS.

References

Asanuma, H., Takayama, J., Niitsuma, H., 2001 “Discrimination of coherent waves by a time-frequency representation of 3D hodogram and application to microseismic reflection method”, *SEG Expanded Abstracts*, 20, 424-427.

Asanuma, H., Izumi, T., Kumano, Y., Soma, N., Niitsuma, H., Baria, R., Michelet, S., 2004 “Data acquisition and analysis of microseismicity from simulation at Soultz in 2003 by Tohoku University and AIST, Japan,” *Trans. GRC*, 28, 187-190

Asanuma, H., Kumano, Y., Hotta, A., Niitsuma, H., Schanz, U., Haring. M., 2007. “Analysis of microseismic events from a stimulation at Basel, Switzerland.” *Trans. GRC*, 31, 265-270.

Moriya, H., Nagano, K., Niitsuma, H. 1994 “Precise source location of AE doublets by spectral matrix analysis of triaxial hodogram”, *Geophysics*, 59, 36-45.

Niitsuma, H., Moriya, H., Nagano, K., 1995 “Calibration method using the spectral matrix for downhole triaxial seismic detectors”, *Acoustic Emission*/Microseismic Activity in Geologic Structures and Materials, 19, 611-624.

Reshetnikov, A., Kummerow, J., Shapiro, S. A., Asanuma H., Häring, M., 2011, “Using microseismicity to image the structure of the Basel geothermal reservoir,” Proc EAGE.2011 Annual Mtg., (in-press)

Soma, N., Niitsuma, H., Baria, R. 2002, “Evaluation of Subsurface Structure at Soultz Hot Dry Rock Site by the AE Reflection Method in Time-frequency Domain”, PAGEOPH, 159, 543-562.